Proceedings of the 25th International Conference on
Port and Ocean Engineering under Arctic Conditions
June 9-13, 2019, Delft, The Netherlands

Features of determining the ice flexural strength and the elastic modulus based on floating cantilever beam tests

Evgeny B. Karulin[1, 3], Aleksey V. Marchenko[2], Aleksandr N. Sakharov[4],
Marina M. Karulina[1], Peter V. Chistyakov[4], Dmitry A. Onishchenko[5]
[1]Krylov State Research Centre, St.-Petersburg, RUSSIA
[2]The University Centre in Svalbard, Longyearbyen, NORWAY
[3]State Marine Technical University, St.-Petersburg, RUSSIA
[4]Lomonosov Moscow State University, Moscow, Russia
[5]Gazprom VNIIGAZ LLC, Russia

ABSTRACT

One of the methods to determine the flexural strength of ice and its effective elastic modulus is loading tests of floating cantilever ice beams. This is a practical and relatively simple approach enabling researchers to test ice beam samples representing natural distribution of temperature and salinity in ice cover. The results of such experiments in field conditions have been discussed in many references and, as noted by a number of authors, this testing technique typically involves stress concentrations at the root of ice beam samples, which is a problem for test data interpretation and may potentially result in conservative estimates of the ice flexural strength. In this case, it is meant that stresses, primarily tensile stresses, rise to exceed the stresses calculated based on the beam approach. The level of stress concentration strongly depends on the cuts shaping the sides of cantilever ice beams. Results obtained by various researchers (including those generalized by Timko and O'Brien, 1994) are difficult to compare because of this significant factor. This paper contains results of experimental studies regarding the influence of beam root details on the test results. The original experiments were conducted in fresh-water ice, which in the authors' opinion, provides the best description of the effect under consideration. In addition to experimental data, the paper presents the results of 3D modeling of the cantilever ice beams with various clamp options. The data were generalized to suggest a shape option for the cantilever ice beam, which significantly reduces the impact of stress concentrations on the flexural strength estimates. With regard to the elastic modulus, the performed study showed that its value can be appropriately determined based on the cantilever beam curvature.

KEY WORDS: Flexural strength; Cantilever beam; Stress; Concentrations, Elastic modulus

INTRODUCTION

Ice strength properties have to be determined for estimating stability of ice-resistant structures on seabed, ice-going capability of vessels, i.e. when problems associated with ice

failure processes are addressed. One of the parameters characterizing the strength of continuous level ice is its flexural strength. This quantity can be determined in different ways. One method is to load a floating cantilever ice beam until it breaks. It is a practical and relatively simple approach enabling experiments on ice specimens with natural temperature and salinity distributions. One of the advantages of this method is that the obtained result is valid across the full thickness of ice. Such experiments and their results have been described in many publications (Dykins, 1968; Frederking and Svec, 1985; Frederking and Hausler, 1978; Tatinclaux and Hirayama, 1982). In-situ full-scale tests on flexural strength of floating cantilever beams have been performed in the Van-Mijen Fjord and Ice Fjord of Spitsbergen fjords since 2009 (Karulin et al., 2011; Karulina et al., 2013; Ervik et al., 2014; Marchenko et al., 2017).

Svec et al. (1985) have noticed one specific feature of this method, namely, stress concentrations arising at ice beam roots, which cause problems for interpretation of test data and may result in underestimation of the flexural ice strength. Svec et al. (1985) also give the results of numerical simulation of a two-dimensional bending of cantilever beam and experimental data on stress distribution around stress-relieving holes at the root of side cuts. The experiments were performed using the photoelastic method. It was shown that the stresses near the beam root decrease with the increase of the hole diameters. Marchenko et al (2014) analyzed three-dimensional effects of local increase of axial stress near the root holes in the tests with floating cantilever beams and discussed potential influence of underestimation of the flexural ice strength on ice failure by waves.

Frederking and Svec (1985) compared the results obtained from cantilever ice-beam bending simulations with the flexural strength data determined experimentally based on the beam theory relationships. The modulus of elasticity was also determined in these experiments based on the ice-beam strain. The tests were conducted in an outdoor manoeuvering basin filled with freshwater. For quite warm freshwater ice (mean temperature not lower than -2°C), the correction factor was obtained. At the same time, Timco (1985) found that, in the case of sea ice with a temperature not lower than -10°C, there was no influence of the stress relief holes at the root on the tests results.

In this paper the results of full-scale tests on bending of floating cantilever beams performed with different diameters of stress-relieving holes at the beam roots are discussed and analyzed. The local rise of primarily axial stresses in an ice beam is compared with stresses acting in the longitudinal plane of symmetry at the same cross section of the beam, at maximum distance from its neutral plane. Deformations of floating cantilever beams are compared with the deformations calculated from simple beam theory approach. An influence of deformations near the root of a floating cantilever beam on a methodic of calculation of the effective elastic modulus is discussed. The modified geometry of a floating cantilever beam is considered, which allows avoiding the effect of increasing local stress in the beam root on the flexural strength.

DESCRIPTION OF EXPERIMENTAL PROCEDURES

Test setup and equipment

A short series of tests on floating cantilever ice beams was carried out at a freshwater lake located on the slope of Breinosa Mountain, outside Longyearbyen (Svalbard), during the autumn of 2014 (late October-early September). The main purpose of these experiments was to find out how the obtained flexural ice strength values depend on the diameter of stress-relieving holes at the root of side cuts (Figure 1). Concurrently, deflections of the ice beam tip under load were determined to estimate the effective modulus of ice elasticity. Stresses at

break of cantilever beams and the effective modulus of elasticity were estimated based on the simple beam theory:

$$\sigma_f = \frac{6F_b \cdot l}{bh^2}; \qquad E = \frac{F_b}{\delta_b} \cdot \frac{4l^3}{h^3 b} \tag{1}$$

where F_b is the breaking force; δ_b is the deflection of the free end of the beam at the moment of its breakage; l, b, h are the length, the width and the ice thickness of a beam, respectively.

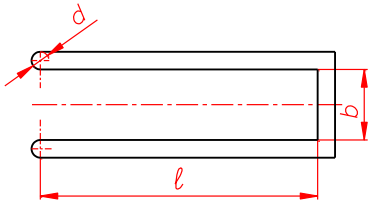

Figure 1. Cantilever beam (planform) and stress relief holes of diameter d

The flexural strength of ice was determined by traditional cantilever beam test procedures as per ITTC recommendations (ITTC, 2014) using the following equipment (Figure 2b):

- loading steel frame mounted over the free end (tip) of cantilever beam to transmit forces from fixed ice to the beam (1);
- tensioning chain anchors to fix the loading frame on ice surface (7);
- electro-hydraulic station and hydraulic cylinder (4);
- strain gauge dynamometer (3) and displacement transducer (5) fixed to strut (6);
- data logger unit (8) to measure and record signals from the dynamometer and displacement sensor.

a). Beam side cutting

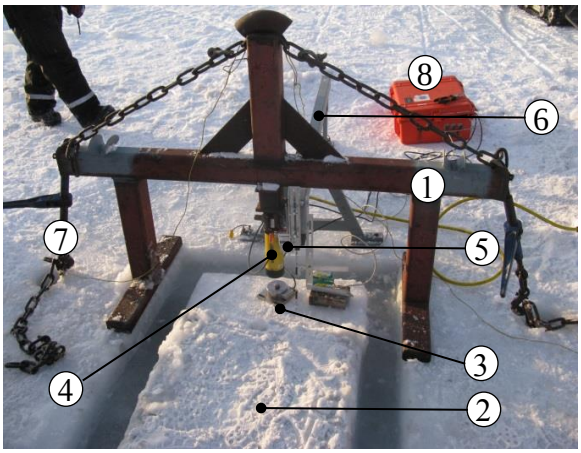

b). Loading schematic

c). Beam root with 100 mm holes

d). Beam root with 200 mm holes

Figure 2. Test equipment and beam preparation. Ice Fjord, February 2010

The cantilever beam was cut from the ice cover, and the vertical holes of specified diameter

were drilled at the clamped beam end (Figure 2a,c,d). The snow cover effect on flexural strength was not investigated. For the purpose of static balance, snow on the cantilever ice beam was left untouched. However, the clamped end was cleared of snow to observe cracking.

During the tests, the force applied to the beam and the beam's tip deflection were recorded (sampling rate 50 Hz). The beam deflection was measured with respect to unloaded ice surface around the loaded tip (at the point on the opposite side of Π-shaped cut). Figure 3a,b gives sample records of the load force and beam tip deflection. In the cases under consideration ice failure happened very quickly (<1.5 s), and it can be assumed that it was a brittle failure. This is what makes the results of this experimental study essentially different from those obtained by Frederking and Hausler (1978).

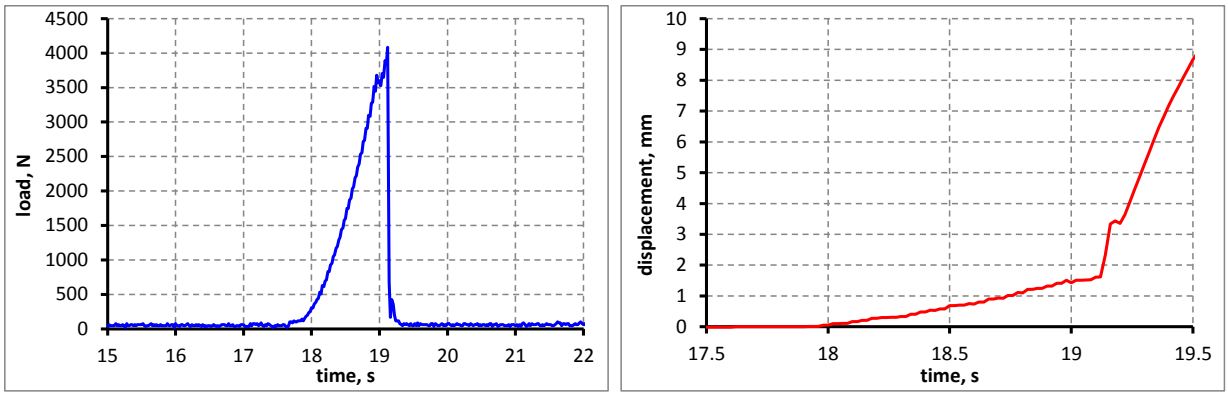

a). Time series of beam loading

b). Time series of beam tip deflection

Figure 3. Sample records

Experimental results

The processed test data are summarized in the Table below. Figure 4a and Figure 4b graphically show the flexural strength and effective modulus of elasticity versus the diameter of holes at the root-end of side cuts.

Table 1. Results of the field works

No	Date	Length l [m]	Width b [m]	Thickness h [m]	Temperature [° C]	Flexural strength [kPa]	Deflection [mm]	Young module [MPa]	Root diam d [mm]
1.	25.10.2014	1.80	0.60	0.26	-0.1	508	1.10	3831	100
2.	28.10.2014	1.45	0.6	0.27	-1.0	428	0.80	2767	100
3.	29.10.2014	1.46	0.6	0.28	-1.2	664	1.70	1985	350
4.	30.10.2014	1.66	0.6	0.28	-0.1	497	0.80	4060	50
5.	01.11.2014	1.72	0.58	0.3	-0.5	807	1.62	3278	200

The data presented in Figure 4a indicate that at smaller diameters of holes at the root-end of side cuts the ice beam specimens break at lower stresses as calculated from the simple beam theory. It is likely that the failure is initiated at the locations where stresses exceed the stress level calculated by the simple beam theory. This is due to specific shape features of the side cuts at the beam root, which act as stress raisers (concentrators). Figure 4b indicates that the beam tip deflection is changed with the hole diameter variation. At the same time we assume that the ice effective elastic modulus is constant as a certain medium parameter.

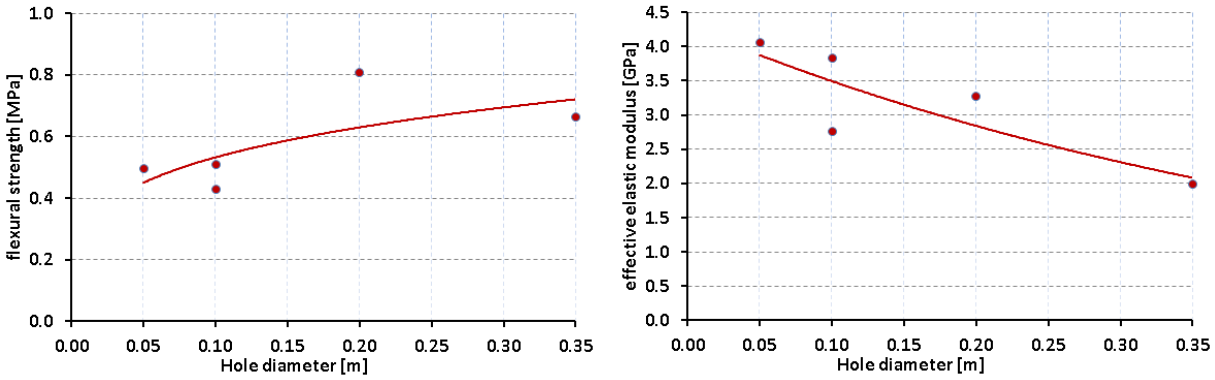

a) b)

Figure 4. Flexural strength (a) and effective elastic modulus (b) of freshwater ice versus the diameter of holes at the beam roots (experimental points and best fit lines)

Numerical simulations of the above-described experiments were performed for in-depth analysis of the obtained data.

NUMERICAL SIMULATION

Statement of problem, co-ordinate axes, computational domain, computational grid

For interpretation of the obtained experimental results numerical simulations were performed to address the problem of cantilever ice beam bending. Beams were assumed to be cut out from a freely floating ice plate and sized as the ice beams used in the physical experiment. Computations were performed by Comsol software.

Simulations were done for a homogeneous isotropic plate of constant thickness resting on elastic foundation. The co-ordinate axes have their origin on the lower beam surface at intersection of the beam symmetry plane and the plane passing through the vertical axes of root holes. OX-axis is directed along the beam symmetry plane and positive from the beam root to the beam tip, OY-axis is positive to the left of the positive OX-axis direction, OZ-axis is positive upward. For keeping the equilibrium condition similar to that of the in-situ experiment, the vertical load, which is applied to the vertical face of the tip to bend the beam, is counterbalanced by an opposite and equal force applied to the hole simulating anchor holes 7 (Figure 2b). The material is assumed to be of a linearly elastic type. It is assumed that the ice beam is cut out from a circular plate of 100 m diameter and 0.28 m thickness (Figure 5a). Horizontal displacements of beam's side surface are assumed to be 0. The problem is solved as a symmetric problem with respect to the beam's vertical plane of symmetry. A domain in the vicinity of the beam is identified to generate a finer computational grid (Figure 5b). A small area near the beam is represented by prismatic finite elements with triangular bases, while a wider area is represented by tetrahedral elements. The total number of finite elements range from 110000 to 140000, depending on the domain configuration. The following environmental constants are assumed: modulus of elasticity E – 3.2 GPa, ice density ρ_{ice} – 900 kg/m^3, Poisson ratio – 0.36, water density ρ_w – 1025 kg/m^3, stiffness of elastic foundation – $\rho_w \cdot g$, where g is the gravitational acceleration. Environmental parameters are similar to the real ice parameters in the in-situ experiment. The beam was statically loaded with a force whose magnitude was close to the in-situ test force of 1300 N applied to half of the beam (due to the problem symmetry).

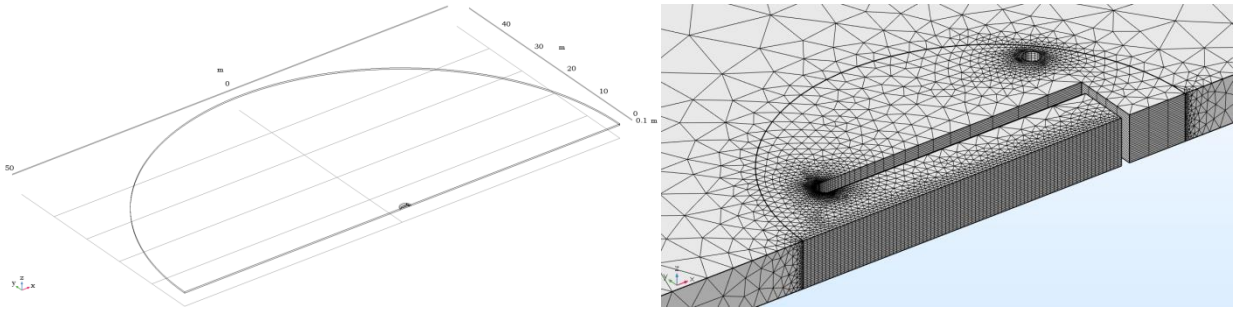

a) b)

Figure 5. Computational domain and grid

Computational cases. Results of computations

Dimensions of ice beams chosen for numerical simulations are given in Table 2.

Table 2. Ice beam dimensions in numerical simulations

No	**Length ℓ [m]**	**Width b [m]**	**Thickness h [m]**	**Root diameter d [m]**
1	1.600	0.600	0.280	0.050
2	1.600	0.600	0.280	0.100
3	1.600	0.600	0.280	0.200
4	1.600	0.600	0.280	0.350

Figure 6 gives distributions of stresses $\boldsymbol{\sigma_{xx}}$ along the following lines: Figure 6a – distribution along longitudinal lines on the upper surface (z=0.28 m) and lower surface (z =0.00 m) of the beam, at mid-length of the beam (y=0.00 м), at 0.25 width (y=0.15 m) of the beam, and at the beam edge (y=0.30 m); Figure 6b – distribution along transverse lines in two cross sections, at different distances from the co-ordinate axes origin (x=-0.010, x=0.000 and x=0.010 m) at mid-height of the beam (z=0.14 m), at 0.75 height of the beam (z=0.21 m), and on the upper surface of the beam (z=0.28 m).

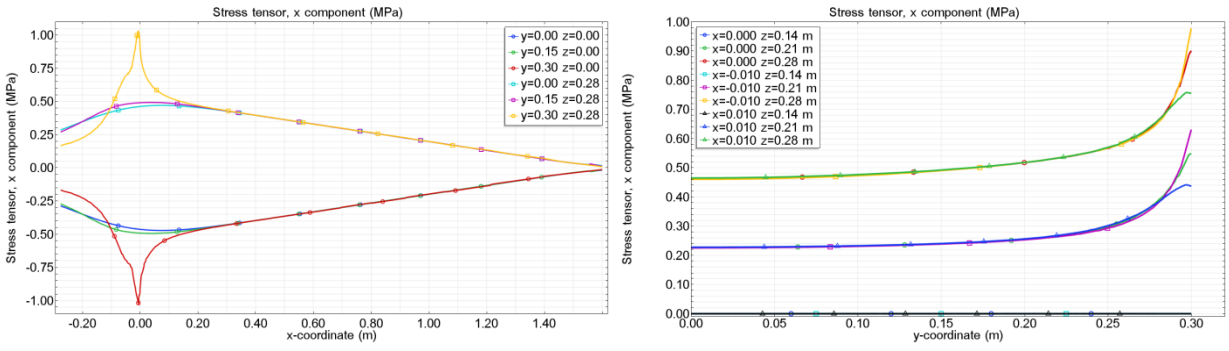

a) b)

Figure 6. Longitudinal and transverse distribution of stresses $\boldsymbol{\sigma_{xx}}$

Stress data computations were analyzed based on tensile stresses $\boldsymbol{\sigma_{xx}}$ taken at the following points: σ_{xx}^{E} is the maximum tensile stresses on the beam side near its root, at the point where the cylinder shape transits to flat side surface (point A in Figure 7a); σ_{xx}^{M} is the maximum tensile stresses on the line where the upper beam surface is crossed by the plane of beam's symmetry (the point is located near the plane passing through vertical axes of root holes, point B in Figure 7b).

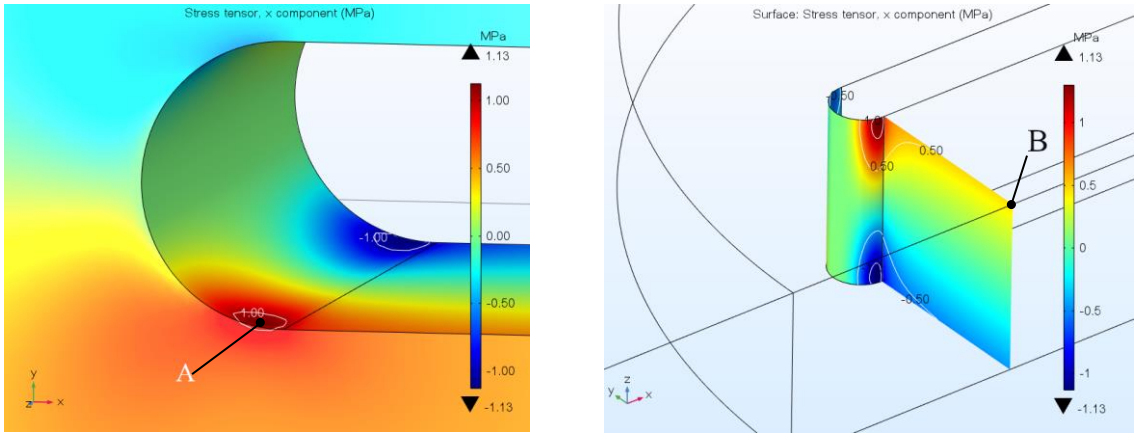

a) b)

Figure 7. Distribution of stresses $\boldsymbol{\sigma_{xx}}$ for the beam with root holes of d=100 mm

The stresses obtained for the above-said characteristic points are given in Table 3. It is seen from the given results that:

- Maximum stresses on beam's side surface around the stress concentrator are decreased as the root hole diameter is increased;
- Maximum stresses on beam's upper surface in the longitudinal plane of symmetry near root are increased as the root hole diameter is increased.

The latter is understandable because the system tends to hold its balance.

The same table contains the values of coefficient: $K = \boldsymbol{\sigma_{xx}^M / \sigma_{xx}^E}$ – ratio of upper surface stresses to side surface stresses near the stress concentrator. Figure 8 shows the coefficient K in function of the root hole diameter. The curve has the same pattern as the curve in Figure 4a, above. Presumably, this fact can be employed to take into account the effect of root hole diameters on the estimated flexural strength of ice. This approach was implemented by Frederking and Svec (1985).

Table 3. Tensile stresses in characteristic beam points

No	**Root diameter d, m**	**Maximum stresses on beam's side surface σ_{xx}^{E}, MPa**	**Maximum stresses on upper surface at beam's mid-width σ_{xx}^{M}, MPa**	$K = \frac{\sigma_{xx}^{M}}{\sigma_{xx}^{E}}$
1	0.050	1.350	0.450	0.333
2	0.100	1.030	0.462	0.449
3	0.200	0.837	0.480	0.573
4	0.350	0.730	0.495	0.678

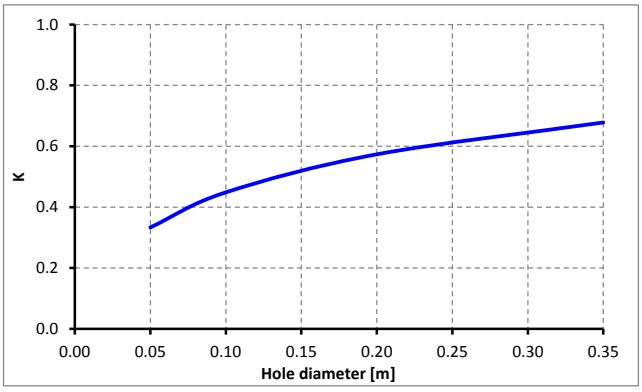

Figure 8. Parameter $K = \boldsymbol{\sigma_{xx}^M / \sigma_{xx}^E}$ vs. the hole diameter

Numerical results were also used to check if the effective modulus of elasticity was correctly "reconstructed" based on the simple beam theory for the cantilever beam and the beam tip deflection measurements. For this purpose deflections in 4 points were determined on the beam upper surface in the longitudinal plane of symmetry (Figure 9): point No. 1 on beam tip; point No. 2 on opposite surface of side cut; point No. 3 on plane of root hole axes (x=0.000 m); point No. 4 on plane tangent to the remotest points of root holes (x=-0.5*d m).

Figure 9. Layout of points for beam deflection measurements

Table 4 gives deflections, deflections differences, and effective elastic modulus of ice estimated using the difference between deflections in relevant points. The same table contains the results of computations done for the same beam based on the assumption that the beam cross section at the origin of co-ordinate axes is fully fixed. This section passes through vertical axes of root holes. This case is marked in the table by *.

Table 4. Deflections of characteristic beam points and effective elastic modulus

Root diameter d, m	**Point deflection, mm**				**Difference in point deflection, mm**			**Effective elastic modulus corresponding to deflection difference, GPa**		
	№ 1	№ 2	№ 3	№ 4	№ 2-№ 1	№ 3-№ 1	№ 4-№ 1	№ 2-№ 1	№ 3-№ 1	№ 4-№ 1
0.050	2.138	0.131	0.333	0.333	2.006	1.804	1.804	1.61	1.79	1.79
0.100	2.278	0.134	0.380	0.354	2.145	1.899	1.925	1.51	1.70	1.68
0.200	2.522	0.134	0.462	0.403	2.388	2.060	2.119	1.35	1.57	1.53
0.350	2.857	0.124	0.587	0.468	2.733	2.270	2.389	1.18	1.42	1.35
0.100*	1.001	0.000	0.000	0.000	1.001	1.001	1.001	3.23	3.23	3.23

It is seen from the table (rows 1-4) that computations of the effective elastic modulus based on the simple beam theory yield very low values. The reason is not only deflection of the beam root, but also rotation of the cross-section at the same place. Figure 10 illustrates this issue. Even if the modulus of elasticity were to be estimated from the difference in deflection of beam's tip and root (Figure 10 dashed line), there would be a significant error due to an angle of rotation at the root section.

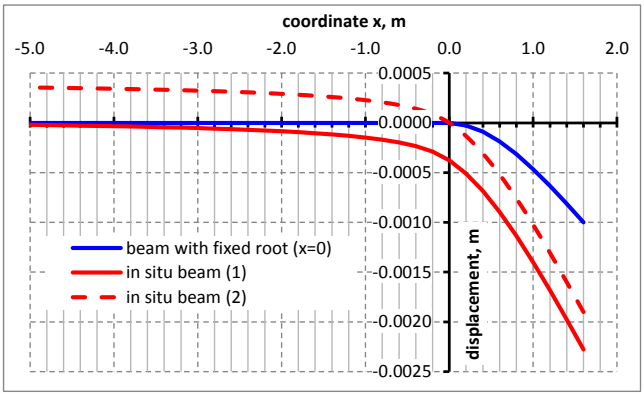

Figure 10. Comparison of bending behavior of a beam modelled from field tests and that of the same beam with a fixed root section (root diameter 0.1 m): the solid red line (1) – deflection of the beam root and rotation of the cross-section in the root; the dashed red line (2) – only rotation of the cross-section in the root

Determination of effective elastic modulus based on the curvature of the beam

In accordance with Timoshenko and Goodier (1970), the elastic modulus distribution along the beam can be calculated as $E = \frac{M(u)}{k(u) \cdot J}$ where u is the coordinate according to Figure 11, $u = l - x$; $M(u)$ is bending moment; $k(u)$ is the curvature of central line of the beam determined as $k(u) = \frac{d\varphi(u)}{ds}$; φ is the sloping angle of the central line to horizon; s is a coordinate along the central line; and $J = \frac{bh^3}{12}$ is the inertia moment of the beam cross-section.

If the curvature is small, then $ds \cong du$. For a cantilever beam $M(u) = Fu$, and the curvature depends linearly on u, i.e. $k = Au$. For calculation of parameter A, measurements of the central line deflection $\{w_{i-1}, w_i, w_{i+1}\}$ at three points $\{u_{i-1}, u_i, u_{i+1}\}$ can be used (Figure 11):

$$A = \frac{6}{(u_{i+1}-u_{i-1})(u_{i+1}+u_i+u_{i-1})} \cdot \left(\frac{w_i-w_{i-1}}{u_i-u_{i-1}} - \frac{w_{i+1}-w_i}{u_{i+1}-u_i}\right) \quad (2)$$

The elastic modulus is calculated as

$$E = \frac{F}{AJ}. \quad (3)$$

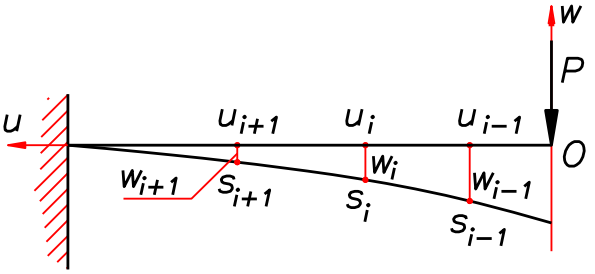

Figure 11. Scheme for determination of elastic modulus based on the beam curvature

The method was applied for determination of the elastic modulus in the numerical case presented above (Figure 10, blue line). Table 5 contains the results of calculations. It can be seen from the table that the calculated values of the elastic modulus are close to the predetermined value of E=3.2 GPa (the discrepancy is less than 1%).

Table 5. Calculation of the elastic modulus (Eqs. 2 and 3)

u-coordinate, m	0.0	0.5	1.1	1.6
Deflection w, m	-0.00227780	-0.00153992	-0.00078566	-0.00037636
Parameter A, m^{-2}	-	0.000745488	0.000747471	-
Elastic modulus E, GPa	-	3.178	3.169	-

This result confirms the validity of the described method. It can be used in the field tests for determination of the effective elastic modulus based on the deflection measurements at several points (≥ 3) along the cantilever beam length. The similar approach based on the least-squares deviation method was suggested by von Bock and Polach (2005) for model ice.

MODIFICATION OF CANTILEVER BEAM PLANFORM TO MITIGATE STRESS CONCENTRATION EFFECT ON THE FLEXURAL STRENGTH EVALUATIONS

In order to obtain correct flexural strength of ice it is possible to:

- introduce some correction factors allowing for stress concentrator effects;

- adjust the beam shape to eliminate stress concentration effects on the beam failure process.

The first option is flawed by uncertainty as to how the correction factors depend on the beam geometry and ice properties. The above-described experiments in freshwater ice have revealed that stress concentrations influence the flexural strength values. At the same time, Frederking and Svec (1985) have not found that kind of effects in seawater ice experiments. This study attempts to follow the second option, i.e. to modify the beam planform so that ice would not fail in the area of stress concentrations, but under smooth change of the beam form where stress variations are described by the simple beam theory. Figure 12a shows suggested Y-shape planform of the beam, which has a radial transition of parallel side surfaces to a wider base near the root.

Table 6 gives parameters of the tested Y-shape cantilever beam and the determined flexural strength values. The beam's view before and after the failure is shown in Figure 13. It can be seen that the beam failure took place at some distance from the root, and the obtained flexural strength was greater than the value determined from the test with the beam of traditional planform (Table 6, second row). Both beams had the stress relief holes of same diameter in the root section.

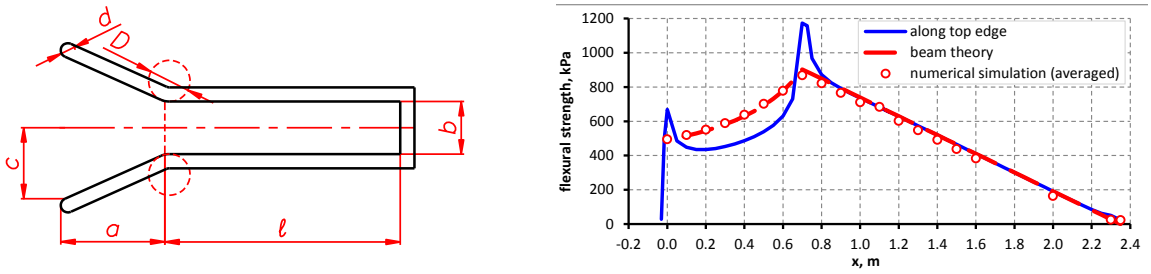

a) b)

Figure 12. Y-shape beam: a) plan view, and b) flexural stress distribution along the beam

Table 6. The beams geometry and the flexural strength

Type	Length ℓ [m]	Width b [m]	Thickness h [m]	Root diameter d [m]	Conjunction diameter D [m]	Distance a [m]	Distance c [m]	Flexural strength [kPa]
Y-shape	1.650	0.370	0.400	0.100	0.29	0.700	0.300	534
Conventional	1.850	0.495	0.395	0.100	-	-	-	349

a) b)

Figure 13. Y-shape beam before (a) and after (b) the test.

Figure 12b shows distribution of the tensile stresses on the upper surface of the Y-shape beam. The solid red line shows the stress distribution along the beam's axis based on the simple beam theory. The red circles refer to the numerical calculations: these points correspond to the stresses averaged over a width of the beam cross-section. The solid blue line gives the stress distribution along the edge of the beam. Thus, two issues should be considered at modifying the beam planform: 1) the stresses in the root section including the stress concentration effects should be less than the stresses in the other cross-sections, and 2) a smooth conjugation of the planes forming the side surfaces of the Y-shape beam should be used to minimize the stress concentration at those areas. According to the numerical simulations, the stresses increase by 40% at D=0.29 m, by 12% at D=2 m, and by about 4% at D=4 m for the beam shown in Figure 12b.

CONCLUSIONS

The paper gives results of the freshwater ice flexural strength determination based on the cantilever beams bending *in-situ* at various holes diameters at the beam root. As well, the influence of the stress relief hole diameter on the result was studied numerically using 3D FE model. Comparison of the tests results and numerical simulations are in good qualitative agreement regarding the influence of the holes diameters on the flexural strength value determined from the cantilever beam tests. Based on the performed analysis, a modification of the beam planform has been suggested which should eliminate the influence of the holes diameter on the test result.

The performed numerical simulations have indicated systematic error in determination of the effective elastic module based on the cantilever beam tests and the simple beam theory. The error is caused by difference in the deformation processes during bending of the cantilever beam with fixed root and the beam cut from the floating plate. This results in underestimation of the effective elastic module of the ice at about two times due to incorrect application of the simple beam theory to processing the cantilever beam tests data.

The study showed that the determination of the elastic modulus based on the beam curvature gives the adequate values. To implement this method, it is sufficient to know deflections at three points along the beam central axis.

ACKNOWLEDGEMENTS

The authors wish to acknowledge the support of the Research Council of Norway through the Centre for Sustainable Arctic Marine and Coastal Technology (SAMCoT) and AOCEC project of IntPart program

REFERENCES

Dykins J.E. Tensile and flexure properties of saline ice. 1968. *U.S. Naval Civil Engineering Laboratory Port Hueneme*. California 93041 / USA.

Ervik, A., Høyland, K.V., Marchenko, A., Karulina, M., Kaulin, E., 2014. In-situ experimental investigation of the vertical stress distribution in sea ice covers; a comparison of tensile and flexural strength. *Proc. of the 22th IAHR Symposium on Ice*, Singapore, paper 1113.

Frederking R.M.W. and Svec O.J., 1985. Stress-relieving techniques for cantilever beam tests in an ice cover. *Cold regions Science and Technology* 11: 247-253.

Frederking, R.M.W., Hausler, F., 1978. The flexural behavior of ice from in situ cantilever beam tests. *Proc. of the IAHR Symposium on Ice Problems*, Lulea, Vol. 1, 197-215.

ITTC, 2014 – Recommended Procedures 7.5-02-04-02, Testing and Extrapolation Methods. Ice Testing. *Test Methods for Model Ice Properties*.

Karulin, E.B., Karulina, M.M., Shestov, A.S., Marchenko, A.V., 2011. Investigation of sea ice flexural strength in the fjords of the West Spitsbergen. *Transactions of the Krylov Shipbuilding Research Institute*, 63 (347), 131-142. ISBN 0869-8422.

Karulina, M., Karulin, E., Marchenko, A., 2013. Field investigations of first-year ice mechanical properties in North-West Barents Sea. *Proc. Int. Conf. Port Ocean Eng. Arct. Cond., POAC13-049*, Espoo, Finland, 11 pp.

Marchenko, A., Karulin, E., Chistyakov, P., Sodhi, S., Karulina, M., Sakharov, A., 2014. Three dimensional fracture effects in tests with cantilever and fixed ends beams. *Proc. of the 22th IAHR Symposium on Ice, Singapore*, paper 1178.

Marchenko, A., Karulina, M., Karulin, E., Chistyakov, P., Sakharov, A., 2017. Flexural Strength of Ice Reconstructed from Field Tests with Cantilever Beams and Laboratory Tests with Beams and Disks. *POAC17-177*.

Svec O.J., Thompson J.C. and Frederking R.M.W., 1985. Stress concentrations in the root of an ice cover cantilever: model tests and theory. *Cold regions Science and Technology* 11: 63-73

Tatinclaux, J.-C. and Hirayama, K.-I., 1982. Determination of the flexural strength and elastic modulus of ice from in situ cantilever beam tests. *Cold Regions Sci. Technol.,* 6(1), pp. 37-47.

Timco, G.W. and O`Brien, S., 1994. Flexural strength equation for sea ice. *Cold Regions Science and Technology* 22: 285-298.

Timco, G.W., 1985. Flexural strength and fracture toughness of urea model ice. *Proc. 4th Offshore Mechanics and Arctic Engineering Symposium*, Dallas, Texas, Vol. II, pp. 199-208

Timoshenko, S.P. and Goodier, J.N., 1970. Theory of Elasticity, McGraw-Hill, N.Y., USA

von Bock und Polach, R. F., 2005. Sea ice characteristics and its impact on model tests (master thesis). Berlin: Technical University of Berlin